TOPICAL REVIEW — Silicene

Silicene on substrates: A theoretical perspective*

Zhong Hong-Xia(钟红霞)[a)c)†], Quhe Ru-Ge(屈贺如歌)[a)d)e)f)†], Wang Yang-Yang(王洋洋)[a)g)†], Shi Jun-Jie(史俊杰)[a)], and Lü Jin(吕 劲)[a)b)†‡]

[a)] *State Key Laboratory for Mesoscopic Physics and School of Physics, Peking University, Beijing* 100871, *China*
[b)] *Collaborative Innovation Center of Quantum Matter, Beijing* 100871, *China*
[c)] *Department of Physics, Washington University in St. Louis, St. Louis, Missouri* 63130, *USA*
[d)] *Academy for Advanced Interdisciplinary Studies, Peking University, Beijing* 100871, *China*
[e)] *State Key Laboratory of Information Photonics and Optical Communications, Beijing University of Posts and Telecommunications, Beijing* 100876, *China*
[f)] *School of Science, Beijing University of Posts and Telecommunications, Beijing* 100876, *China*
[g)] *Department of Nuclear Science and Engineering and Department of Materials Science and Engineering, Massachusetts Institute of Technology, Cambridge, Massachusetts* 02139, *USA*

(Received 9 June 2015; revised manuscript received 2 July 2015; published online 20 July 2015)

Silicene, as the silicon analog of graphene, is successfully fabricated by epitaxially growing it on various substrates. Like free-standing graphene, free-standing silicene possesses a honeycomb structure and Dirac-cone-shaped energy band, resulting in many fascinating properties such as high carrier mobility, quantum spin Hall effect, quantum anomalous Hall effect, and quantum valley Hall effect. The existence of the honeycomb crystal structure and the Dirac cone of silicene is crucial for observation of its intrinsic properties. In this review, we systematically discuss the substrate effects on the atomic structure and electronic properties of silicene from a theoretical point of view, especially with emphasis on the changes of the Dirac cone.

Keywords: silicene, dirac cone, substrate effects

PACS: 73.20.–r, 73.40.Ns, 68.35.Ct **DOI:** 10.1088/1674-1056/24/8/087308

1. Introduction

As the silicon analogy of graphene, silicene possesses graphene's both outstanding properties like the Dirac-cone-shaped energy band[1] and the high carrier mobility: theoretically each of silicene and graphene has a carrier mobility on the order of 10^3 cm^2/(V·s)–10^5 cm^2/(V·s),[2,3] and undesirable zero band gap nature.[1] Unlike planar graphene, whose band gap is difficult to open without degrading its electronic property,[4] silicene has a tunable band gap that can be opened in low-buckled silicene (0.44 Å) by a vertical electric field,[5,6] single-side surface adsorption of alkali and transition metal atoms without degrading the electronic properties of silicene.[7,8] Meanwhile, three (p/i/n) doping types are realized for silicene sheets, which can be used to fabricate silicene-based p–i–n transport field effect transistors (FETs).[8] Because of the high carrier mobility, a tunable band gap, and easy integration into the modern Si-base device technologies, silicene is a promising material for high-speed electronic devices, and the silicene-based transistor will own an extremely fast speed, making it able to operate in the THz frequency range.[9] Very recently, a silicene FET operating at room temperature has been realized via growth-transfer-fabrication process, corroborating the expected ambipolar Dirac charge transport.[10]

Due to the stronger spin–orbital coupling (SOC) of Si atom than that of C atom, silicene with an SOC band gap about 1.55 meV (24×10^{-3} meV in graphene)[11] is more eligible in realizing quantum spin Hall effect (QSHE) and fabricating spintronics devices.[12] By adjusting an electric field and/or an exchange field, the QSHE, quantum anomalous Hall effects (QAHE) and valley-polarized QAHE, the quantum valley Hall effect (QVHE), and the valley polarized metal (VPM) state can be realized in silicene,[13,14] providing many potential applications in spintronics and valleytronics. Based on these topological states, spin-filters and spin/valley separators with quite good performance are designed.[15] Therefore silicene serves as an ideal platform for efficiently manipulating spin/valley degrees of freedom.

Unfortunately, silicene is much less stable and more difficult to synthesis than graphene. As is well known that graphene, with sp^2-bonded carbon atoms, can be exfoliated from graphite easily because of the weak van der Waals (vdW) interlayer interactions of graphite. However, silicene, a low-buckled structure with partial sp^3-bonded silicon atoms, can-

*Project supported by the National Natural Science Foundation of China (Grant Nos. 11274016 and 11474012) and the National Basic Research Program of China (Grant Nos. 2013CB932604 and 2012CB619304).

†These authors contributed equally to this work.

‡Corresponding author. E-mail: jinglu@pku.edu.cn

© 2015 Chinese Physical Society and IOP Publishing Ltd

not be exfoliated from bulk silicon due to the strong covalent Si–Si bonds. Thus, the exfoliation technique developed for graphene does not work for silicene. Hence the major method of synthesizing silicene sheet is to epitaxially growing it on solid surfaces. Silicene has been first successfully synthesized by depositing silicon onto Ag (111) substrate,[16,17] and further obtained by segregation on the top of ZrB_2 thin film epitaxially grown on Si wafer,[18] and then by directly depositing silicon atoms onto Ir (111) surface and annealing the sample at 670 K,[19] and being deposited on the ZrC (111) at 800 K.[20] Recently, high-buckled two-dimensional (2D) Si nanosheets (2 Å in thickness) has been fabricated by molecular beam epitaxial growth on bulk MoS_2 surface.[21] Many other substrates, including graphene, Ca, Pb, SiC, BN, MoX_2 (X = S, Se, and Te), WSe_2, and GaS, have been proposed and investigated theoretically.[22–27]

In order to observe the high carrier mobility and various topological properties, the honeycomb crystal structure and the Dirac cone of silicene must be maintained. Therefore, the effects of the substrates on the structural and electronic properties of silicene must be clarified. In this review, we will discuss the properties of silicene on various substrates. Special attention will be paid to whether the key Dirac cone of free-standing silicene can be preserved on substrate. The reviewed substrates generally satisfy two criteria: hexagonal symmetry lattice and a small lattice mismatch (Δa) with silicene. This review is organized into the corresponding two sections as follows. In the first section, we discuss the electronic properties of epitaxial silicene layers on Ag, ZrB_2 (ZrC), Ir, and other metallic substrates. Due to enhanced band hybridization, the absence of the Dirac cone is a common characteristic for silicene on metal substrates, except for graphene, Ca, and Pb. On these three metal surfaces, supported-silicene can preserve its intrinsic Dirac cone below the Fermi level (E_f). In the second section, silicene layers on insulating and semiconducting 2D layered substrates, including SiC, BN, MoX_2 (X = S, Se, and Te), WSe_2, GaS, and other non-metallic substrates are summarized. It is found that the lattice mismatch and work function play crucial roles in the electronic properties of silicene on non-metallic substrates.

2. Silicene on metallic substrates

Because silicene does not exist in nature, we must evaporate and deposit Si atoms on substrates (or templates) to synthesize it. The major method of synthesizing silicene is to epitaxially growing it on metallic substrates, and this method has been used up to now. For instance, silicene has been successfully grown on metallic Ag, ZrB_2,[18] Ir,[19] and ZrC[20] substrates. Additionally, silicene must contact metal electrodes in real device applications. Understanding the nature of silicene on metallic surface will pave a way for investigating other important physical phenomena such as superconductivity.[28–30] Many efforts thus have been devoted to both theoretical and experimental researches of silicene on metals. According to the periodic table, we focus on the researches of fcc metals with (111) surfaces and hcp metals with (0001) surfaces because of their hexagonal symmetry, which are indicated by brightness in Fig. 1.[22]

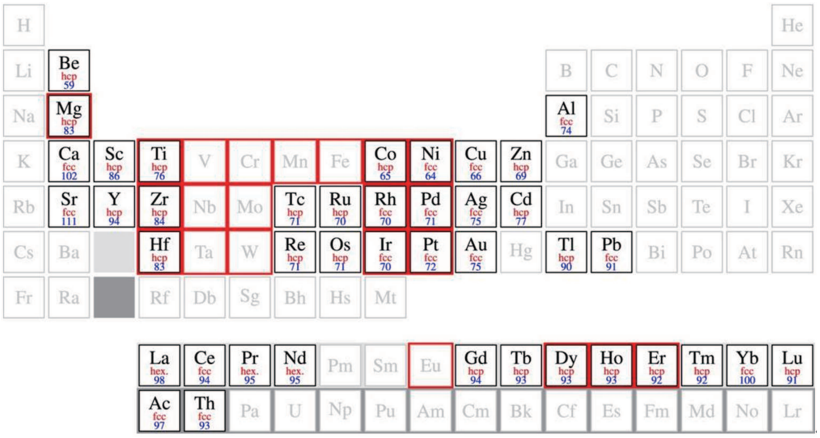


Fig. 1. (color online) Periodic table. The metals with fcc and hexagonal structure are indicated. The corresponding (111) or (0001) surfaces have hexagonal symmetry. The crystal structure is indicated (in red), while the relative lateral lattice constant compared with that of silicene is given as a (blue) number in per cent. The elements in red squares form silicides. Reproduced with permission from Ref. [22] (Copyright 2014 Institute of Physics).

2.1. Silicene on Ag (111) surface

Among all the metallic substrates, Ag is the most common substrate to synthesis silicene experimentally because of the moderate and homogeneous interaction, and good lattice match between Ag (111) surface and silicene.[31] Several phases of silicene have been successfully fabricated by epitaxial growth on Ag (111) with superstructures of

(3×3)silicene/(4×4)Ag (111),[16,32–35]

(2×2)silicene/$(\sqrt{7}\times\sqrt{7})$Ag (111),[32]

$(\sqrt{7}\times\sqrt{7})$ silicene/$(2\sqrt{3}\times 2\sqrt{3})$ Ag (111),[17,32,35,36]

$(\sqrt{7}\times\sqrt{7})$ silicene/$(\sqrt{13}\times\sqrt{13})$ Ag (111),[32,34,35]

and

$\sqrt{3}\times\sqrt{3}$ silicene[37,38]
as shown in Fig. 2.[32]

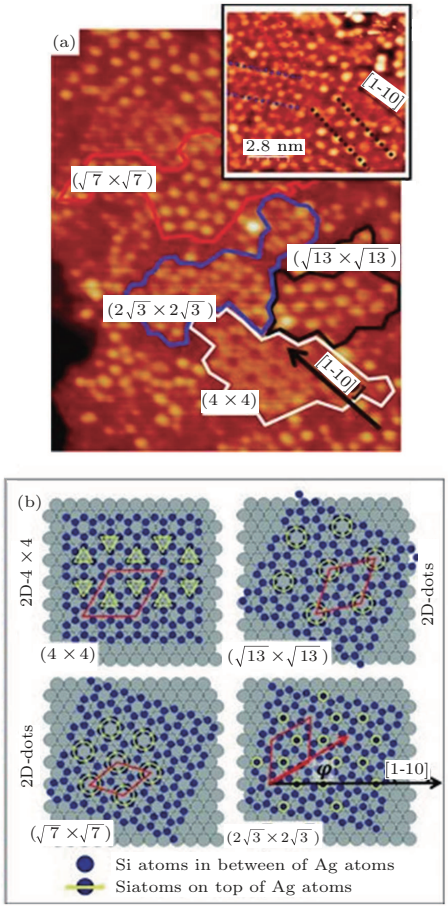


Fig. 2. (color online) STM characterization of multi-oriented silicene domains on Ag (111). (a) From an STM image, a pictorial view of individual Si domains with patch together to form a larger interconnected sheet. In the inset a different STM image ($V = -1.5$ V, $I = 0.2$ nA) emphasizes the different orientations of the patterned silicene domains; the black arrow indicates the [1–10] direction of the Ag (111) surface, while dotted guidelines (red, blue, and black) distinguish the different preferential orientations of the silicene superstructures. (b) Sequence of ball models which simulate the superpositions of oriented honeycomb silicene lattices (blue spots) on the Ag (111) surface (grey spots); several superstructures are generated by particular orientations of the silicene with respect to the Ag (111) lattice (Reproduced with permission from Ref. [32]. Copyright 2012 Wiley Online Library).

The appearing of different superstructures is attributed to the different substrate temperatures and deposition rates.[35] Among these different superstructures, the phase of (3×3)silicene/(4×4)Ag (111) has attracted most attention due to the small Δa (0.3%). Experimentally, there is a fierce debate over the existence of Dirac cone in silicene on Ag surface. The scanning tunneling microscope (STM) and angle-resolved photoemission spectroscopy (ARPES) results in phases (3×3)silicene/(4×4)Ag (111), which provide an evidence that both structural and electronic properties of the 2D silicene are very similar to those of graphene.[37] Unfortunately, the scanning tunneling spectra (STS) in

(3×3)silicene/(4×4) Ag (111) and
($\sqrt{7}\times\sqrt{7}$)silicene/($\sqrt{13}\times\sqrt{13}$)Ag (111)

phases demonstrate that the two Ag-supported silicene phases have lost their Dirac fermions and 2D characteristics, because no Landau level (LL) sequences peculiar to Dirac electrons appears under a strong magnetic field (Fig. 3(c)) as the LL observed in the highly ordered pyrolytic graphite (Fig. 3(d)).[33]

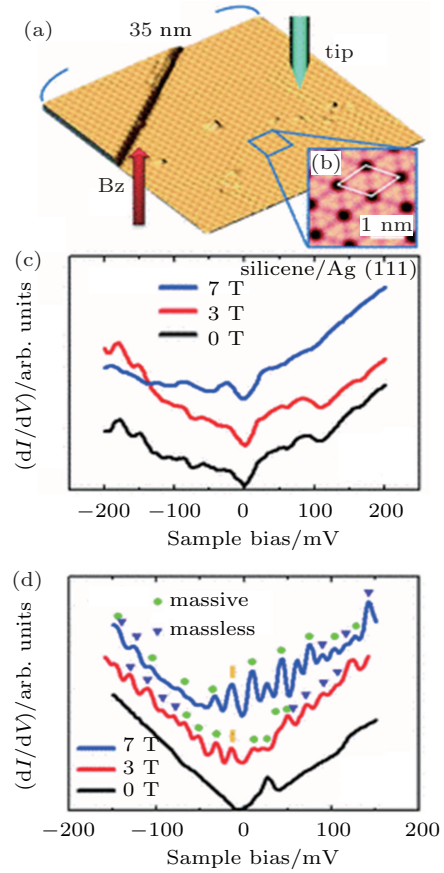


Fig. 3. (color online) (a) STM image of large area of silicene (sample bias voltage $V_s = 0.70$ V and tunneling current $I_t = 0.19$ nA. The image size is 35 nm×35 nm). (b) High resolution STM image of the 4×4 silicene ($V_s = +0.50$ V and $I_t = 0.30$ nA, 3.65 nm×3.65 nm). The unit cell is shown by the white rhombus. (c) The STS spectra of silicene for various magnetic fields perpendicular to the sample surface, B_z. (d) The STS spectra of HOPG for various values of B_z. The purple triangles and green circles show the peaks originating from the LLs of massless and massive Dirac fermions, respectively. The $n = 0$ LL is marked by the yellow bar and the $n = 1$ LL of massive Dirac fermions is not clearly resolved in 3 T due to low magnetic field (Reproduced with permission from Ref. [33]. Copyright 2013 American Physical Society).

Subsequently, extensive theoretical calculations clarify that the Dirac cone in the observed phases of

(3×3)silicene/(4×4)Ag (111),
(2×2)silicene/($\sqrt{7}\times\sqrt{7}$)Ag (111),
($\sqrt{7}\times\sqrt{7}$)silicene/ ($2\sqrt{3}\times2\sqrt{3}$)Ag (111),
($\sqrt{7}\times\sqrt{7}$)silicene/($\sqrt{13}\times\sqrt{13}$)Ag (111)

is severely destroyed by the strong hybridization between silicene and Ag substrates in Figs. 4 and 5.[33,39–46] The experimentally observed Dirac-cone-like features in (3×3)silicene/(4×4)Ag (111) and ($\sqrt{7}\times\sqrt{7}$)silicene/($\sqrt{13}\times\sqrt{13}$)Ag (111) phases are ascribed to the s–p bands of bulk Ag or the silicene-Ag hybridization instead of the intrinsic bands of silicene.

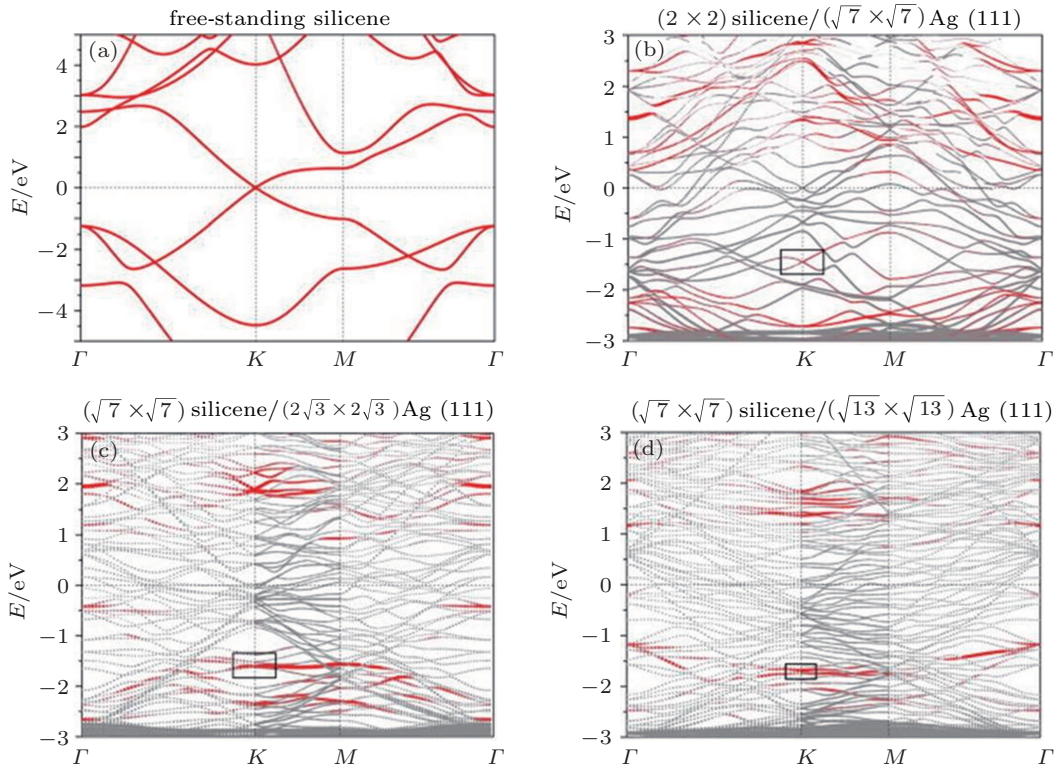


Fig. 4. (color online) (a) Free-standing silicene band structure, in which the π and π^* bands degenerate at E_f. (b) and (c) Projected band structures of silicene/Ag (111) composite systems. Red dots and gray dots represent the states contributed by Ag and Si atoms, respectively. The intensity of the color is proportional to the weight of the corresponding atoms. Black squares indicate those states probably contributed from the π (π^*) bands of silicene. E_f is set to be zero. (For the further implications of color in this figure, the readers can refer to the web version of this article) (Reproduced with permission from Ref. [40]. Copyright 2014 North-Holland).

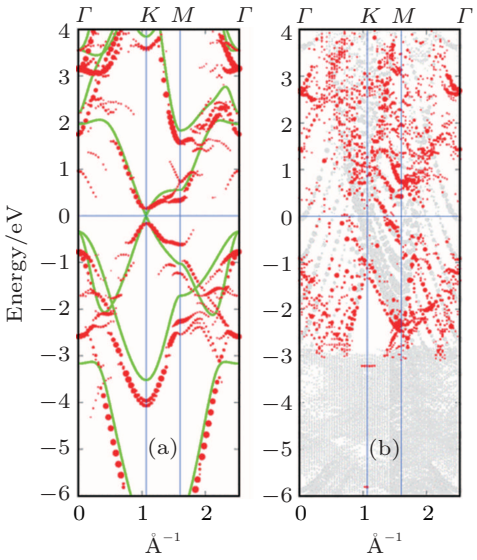


Fig. 5. (color online) (a) Bands of reconstructed (3×3) silicene in the absence of Ag substrate (unsupported silicene) unfolded to BZ of (1×1) silicene, shown by red dots. The radii of dots correspond to the weight of unfolding. The band structure of ideally buckled silicene is shown by green lines. (b) Unfolded band structure of silicene on Ag. Red dots refer to states with significant contribution from silicene (Reproduced with permission from Ref. [39]. Copyright 2013 American Physical Society).

The situation becomes more complicated for the newly found phase of $(\sqrt{3}\times\sqrt{3})$ silicene on Ag (111) surface. Chen *et al.* confirmed the existence of Dirac cone in the phase of $(\sqrt{3}\times\sqrt{3})$ silicene/Ag (111) from the quasiparticle interference patterns (QIP) obtained by STS experiments.[37] The flip–flop motion between the two degenerate $(\sqrt{3}\times\sqrt{3})$ structures explains their hexagonal symmetry STM images at higher temperature and their freezing at lower temperature.[38] However, the evaluated energy barrier for the flip–flop motion (38 meV per Si atom by VASP),[38] is too large to explain the frozen temperature 40 K. Chen *et al.* also argued that the vdW force is crucial to obtaining the rhombic $(\sqrt{3}\times\sqrt{3})$ structure,[38] which is in contrast with the covalent bonds between silicene and Ag in other phases.[42,43] Moreover, the band structure in Chen *et al.* 's paper ignores the interaction between silicene and Ag.[38] By contrast, Guo *et al.* argued that the phase $(\sqrt{3}\times\sqrt{3})$ silicene/Ag is bilayer silicene instead of monolayer (ML) silicene.[47,48] It is the second layer that shows the linear energy dispersions, deduced from the atomic scale STM and on-contact atomic force microscopy (nc-AFM) images.[47,48] This is verified by later theoretical calculations,[49] which indicates that the dispersion (vdW) interactions only play a minor role in the ML silicene/Ag (111) and the energy barriers among the three stable $(\sqrt{3}\times\sqrt{3})$ structures are in a range of 7 meV–9 meV per Si atom. The linear energy dispersion reported in the Chen *et al.*'s experiments[37] corresponds to the silicene–Ag orbital hybridization and shifts downwards deeply in the valence band.

Although it is controversial whether the Dirac cone is present for Ag-supported silicene in experiments, most the-

oretical calculations reach the consistent conclusion that the Dirac cones of all Ag-supported silicene are severely destroyed by the strong band hybridization between silicene and Ag substrates from the electronic band structure. In Table 1, we present the theoretical structural parameters of hybrid structures, such as supported-silicene buckling (Δ), the vertical distance from the bottom silicene layer to the topmost metal layer (d_0), binding energy (E_b) (per Si atom) required to remove the silicene sheet from the surface, and charge transfer (Q). The various phases of Ag-supported silicene display large Δ of 0.95 Å∼1.65 Å, small d ranging from 1.23 Å∼1.87 Å, E_b of 0.7 eV, and Q of $-0.07|e|$.[40,46,49]

Table 1. Structure parameters of the silicene on various metallic substrates. a is the lattice constants of materials, Δa is the lattice mismatch between substrates and free-standing silicene, Δ is the calculated buckling of metal supported-silicene, d_0 is the equilibrium separation of silicene from various surfaces, E_b is the binding energy (per Si atom) required to remove the silicene sheet from the surface, W is the work function for the clean metal surface, Q is the Mulliken charge per Si atom transferred from silicene to the metal surfaces. In the last column, Yes (No) denotes the existence (absence) of the Dirac cone of silicene. The lattice constant, low (high) buckling, and work function of free-standing silicene are 3.87 Å, 0.44 (2.00) Å, and 4.48 eV, respectively.

	a/Å	Δa/%	Δ/Å	d_0/Å	E_b/eV	W/eV	Q/e	Dirac cone
Ag[40]	2.89	−1.2	1.16∼1.65	1.23∼1.87	0.41∼0.72	4.46	−0.07	No
ZrB_2[51]	3.17	5.0	1.58	–	–	4.61	–	No
ZrC[20]		1.0	1.35	–	–		–	No
Ir[46]	2.71	7.2	0.83	1.95	1.69	5.47	0.13	No
Graphene[27]	2.45	−2.0	0.62	3.30	0.07	4.50	–	Yes
Ca[22]	3.92	1.5	0.69∼0.87	2.00	–	2.87 (bulk)	–	Yes
Pb[23]	3.49	1.0	0.65∼0.74	2.80	0.17	4.25 (bulk)	–	Yes
Mg[46]	3.21	4.1	1.52	1.52	0.39	3.55	–0.21	No
Al[46]	2.86	13.2	0.29	2.12	0.35	4.06	−0.06	No
Cu[46]	2.56	1.0	1.25	1.57	0.86	4.69	−0.04	No
Pt[46]	2.77	9.6	0.33	1.97	1.74	5.82	0.06	No
Au[46]	2.88	14.0	0.21	1.81	0.63	5.09	0.04	No

2.2. Silicene on ZrB_2(0001) and ZrC (111) surface

With high melting point, high hardness, high stability against oxidation, and high electric conductivity, the transition-metal carbides (TMCs) and diborides belong to a group of compounds, which have promising applications to high-temperature ceramics and are highly stable substrates for film growth. Fleurence *et al.* successfully synthesized the phase $(\sqrt{3}\times\sqrt{3})$silicene/(2×2)ZrB_2 (0001) through surface segregation on zirconium diboride thin films grown on Si wafers via epitaxial growth.[18] In contrast to the planar and buckled forms of free-standing silicene, the phase $(\sqrt{3}\times\sqrt{3})$silicene/(2×2) ZrB_2 (0001) is "planar-like" phase, with all but one Si atoms per hexagon residing in the same plane.[50,51] The plane is characterized by a residual buckling of just 0.01 Å, with the remaining atoms protruding at a height of 1.58 Å. This indicates that there is a strong interaction between epitaxial silicene and substrate ZrB_2, so that the Dirac point epitaxial silicene on ZrB_2 is destroyed by the hybridization between Si sp^2 and p_z orbitals, accompanied by the Zr d orbitals.[50,51] Apart from ZrB_2, Aizawa *et al.* have fabricated silicene on ZrC (111) in the same phase $(\sqrt{3}\times\sqrt{3})$ silicene/(2×2) ZrC (0001) with very perfect Δa (1%) compared with the value (5%) for the ZrB_2 case.[20] Like the silicene on ZrB_2, the phase $(\sqrt{3}\times\sqrt{3})$ silicene/(2×2) ZrC (111) is also "planar-like" one, with a residual plane buckling of just 0.01 Å but the remaining atoms protruding at a height of 1.35 Å. No crossing of the π band is observed on E_f, suggesting the absence of expected Dirac cone because of the considerable covalent nature for $(\sqrt{3}\times\sqrt{3})$ silicene/(2×2) ZrC (0001) from theoretical calculations.[20]

2.3. Silicene on Ir (111) surface

Silicene has been successfully fabricated on Ir (111) surface by directly depositing silicon on the Ir (111) surface and annealing the sample at 670 K.[19] Both theories and experiments verify the 2D continuity and buckled structure of silicene on Ir (111).[19,52] The phase $(\sqrt{3}\times\sqrt{3})$silicene/$(\sqrt{7}\times\sqrt{7})$R19.1° Ir (111) possesses a Δ value of 0.83 Å, larger than that 0.44 Å of free-standing one, d_0 of 2 Å, E_b of 1.60 eV, and formation energy of 1.10 eV, indicating the stability and a strong adsorption of silicene on Ir surfaces.[19,46] The strong adsorption originates from the strong hybridization between S $3p_z$ and Ir 5d states through partial density of states (PDOS) analysis.[52] Furthermore, there is a large charge accumulation at the interface between silicene and substrates. Therefore, silicene on Ir (111) loses its original Dirac cone around E_f, leading to a metallic band structure.[46,52]

2.4. Silicene on graphene surface

Owing to the hexagonal symmetry and similar honeycomb lattice constants, the heterosystem silicene/graphene is reasonable to have no imaginary phonon frequency.[27,53–55] Multiple phases of silicene with different orientations rel-

ative to graphene have been calculated with small Δa (0.5%∼2.7%).[27] Among the various phases, we take the phase $(\sqrt{3}\times\sqrt{3})$silicene/$(\sqrt{7}\times\sqrt{7})$graphene in Fig. 6 for example. The corresponding projected band structures clearly show that the Dirac cones of silicene and graphene are well preserved, with nearly unchanged Fermi velocities (on the order of 10^5 m/s) at their Dirac points.[27] More interestingly, the silicene and graphene are weakly p- and n-doped, respectively, because their Dirac cones both slightly shift 0.1 eV above and below E_f, in the phase $(\sqrt{3}\times\sqrt{3})$silicene/$(\sqrt{7}\times\sqrt{7})$ graphene. The doped characteristics are essentially caused by a small quantity of Q ($5\times10^{-4}|e|$) from silicene to graphene, inducing small band gaps for silicene (Γ) (26 meV) and graphene (K) (2 meV).[53] Moreover, a conversion of doping types happens to silicene and graphene (i.e., n-doping graphene is converted into p-doping graphene while p-doping silicene is turned into n-doping silicene), when the d_0 is above some certain value (4.2 Å for phase (2×2)silicene/(3×3)graphene), resulting from the competition between the overlap between electronic states and tunneling energy barrier. Therefore, the effective and tunable self-doping in the heterosystem silicene/graphene provides a great potential for fabricating new p–n junctions.

Like the phase $(\sqrt{3}\times\sqrt{3})$silicene/$(\sqrt{7}\times\sqrt{7})$graphene, both silicene in-between two graphene layers and silicene on ML graphene in different supercells possess the atomic and electronic structures identical with those in free-standing buckled silicene, as a result of the weak vdW interlayer interaction.[54] Meanwhile, the substrate silicene preserves its intrinsic electronic properties well. Therefore, silicene and graphene layers are ideal templates for each other for growth and applications, with a small lattice mismatch and well preserved intrinsic properties.

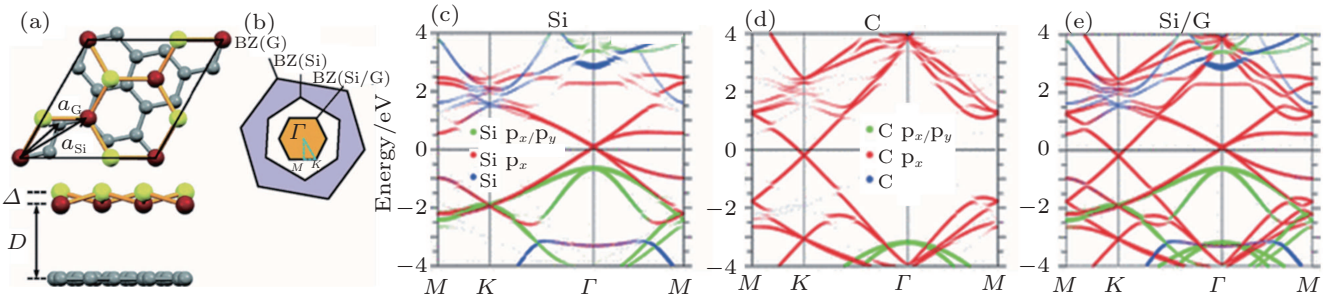


Fig. 6. (color online) (a) Top and side views of the atomic structure of $\sqrt{3}\times\sqrt{3}$ silicene and $\sqrt{7}\times\sqrt{7}$ graphene, where red and yellow atoms represent the two sublattices of Si atoms separated vertically by 0.62 Å, and the grey spheres represent carbon atoms in the graphene layer at a separation of 3.3 Å from the lower silicon layer. The lattice vectors a_{Si} and a_G of the (1×1) unit cell of silicene and graphene, respectively, have a relative rotational angle of 10.9° between them; (b) The first Brillouin zones of the combined system (orange), 1×1 silicene (white), and 1×1 graphene (purple). Band structures of $\sqrt{3}\times\sqrt{3}$ silicene and $\sqrt{7}\times\sqrt{7}$ graphene: (c) the projected states on Si are highlighted; (d) the projected states on C are highlighted; and (e) the projected bands in panels (c) and (d) are combined. The substrate-induced gaps are about 26 meV for Si (Γ) and 2 meV for graphene (K), respectively (Reproduced with permission from Ref. [27]. Copyright 2013 American Physical Society).

2.5. Silicene on other metallic surfaces

The cases of silicene on other promising metals have been predicated theoretically, including

$(\sqrt{3}\times\sqrt{3})$silicene/(2×2)Mg (0001),
$(\sqrt{3}\times\sqrt{3})$ silicene/$(\sqrt{7}\times\sqrt{7})$Al (111),
(1×1)silicene/Ca (111),
$(\sqrt{7}\times\sqrt{7})$silicene/$(\sqrt{13}\times\sqrt{13})$Ti (0001),
$(\sqrt{3}\times\sqrt{3})$silicene/$(\sqrt{7}\times\sqrt{7})$Cu (111),
$(\sqrt{7}\times\sqrt{13})$silicene/$(\sqrt{13}\times\sqrt{28})$Zn (0001),
(3×3)silicene/$(\sqrt{13}\times\sqrt{13})$Zr (0001),
(2×2)silicene/(3×3)Ru (0001),
(4×4) silicene/(6×6)Rh (111),
(3×3)silicene/$(\sqrt{13}\times\sqrt{13})$Cd (0001),
$(\sqrt{3}\times\sqrt{3})$ silicene/$(\sqrt{7}\times\sqrt{7})$Pt (111),
$(\sqrt{3}\times\sqrt{3})$ silicene/$(\sqrt{7}\times\sqrt{7})$Au (111),

and silicene on Pb (111), which are shown in the periodic table (Fig. 1).[22] Owing to the strong silicene–metal hybridization, Dirac cone appears almost in none of all metallic substrates except for Ca and Pb metals.[22,23,46]

Now we first come to discuss the case of silicene on Ca (111) with Δa smaller than 1.5%.[22] Among them, the calculated STM images clearly demonstrates the perfect honeycomb symmetry of silicene on 1×1 Ca (111), and a functionalized Ca(1.0 ML)/(1×1) Si (111), accompanied by Δ values of 0.72 Å and 0.69 Å, respectively. Moreover, the Si p_z-state derived Dirac cones could be identified near the K point for these two substrates as shown in Fig. 7, with corresponding Fermi velocity on the order of 10^5 m/s. Furthermore, band gaps (574 meV and 161 meV) at the Dirac point appear, and the Dirac point is shifted by more than 0.5 eV below E_f.

The other promising metallic substrate to grow and host Dirac fermions is Pb (111) surface, due to its chemical stability to Si and its threefold symmetry.[23] Three silicene superstructures are studied with Δa no greater than 3.0%. The honeycomb structure of silicene is maintained in all cases, with equivalent Δ of 0.65 Å∼0.74 Å, higher d_0 (2.8 Å), lower E_b (0.15 eV), and Q (0.05$|e|$) compared with those for the case of silicene/Ag (111). Consequently, the band structures of the silicene superstructures in Fig. 8 clearly show the original cone-shaped band structures of free-standing

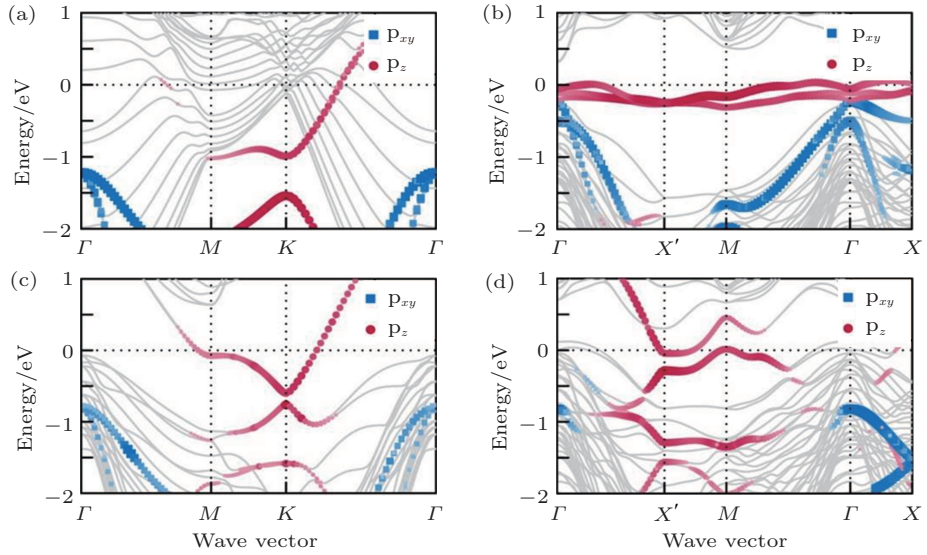


Fig. 7. (color online) Band structures of silicene on (a) Ca (111) 1×1, (b) Ca(0.5 ML)/Si (111) 2×1, (c) Ca(1.0 ML)/Si(111) 1×1, and (d) Ca(1.5 ML)/Si (111) 2×1 surfaces. The silicene p_z (silicene p_{xy}) characteristic of the bands is indicated by red dots (blue squares) of varying size. All bands without silicene characteristics are given by grey lines (Reproduced with permission from Ref. [22]. Copyright 2014 Institute of Physics).

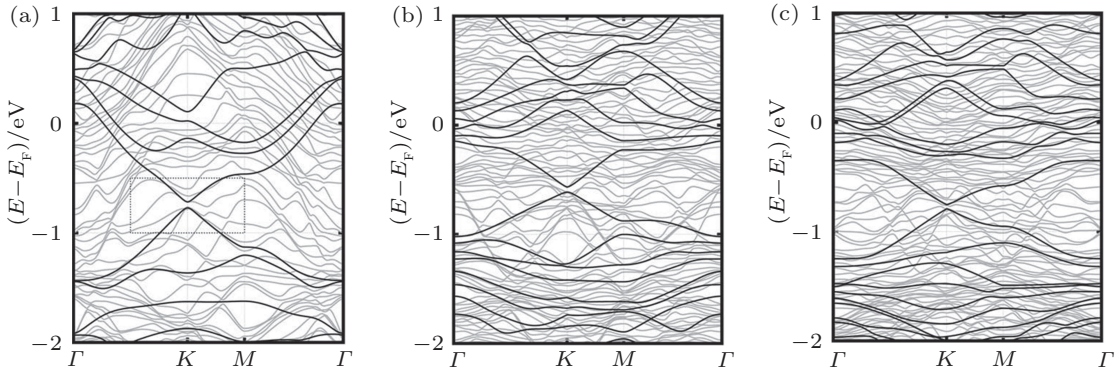


Fig. 8. Band structures of the silicene superstructures (a) $\sqrt{7}\times\sqrt{7}$R19.1°, (b) $\sqrt{13}\times\sqrt{13}$R13.9°, and (c) 4×4 on a Pb (111) surface (light black) and the standalone silicene layer with atoms fixed at their relaxed positions on the surface (dark black). The rectangle in panel (a) denotes the region of the band structure subject to further analysis (Reproduced with permission from Ref. [23]. Copyright 2015 Royal Society of Chemistry).

silicene, which is located at 0.77 eV below E_f, with small gaps of 40 meV∼60 meV. The detailed partial density of states (PDOS) analysis confirms that the Dirac cone has mainly Si 3p orbitals with very little contribution from Pb 6p states, in contrast with the strong hybridization between Si 3p and Ir 5d states. Therefore, the silicene on Pb is predicted to be a massive or gapped Dirac fermions system, like silicene on Ca.

Except for Ca and Pb metals, the severe destruction of the silicene original Dirac cone due to the strong band hybridization between silicene and metallic substrates appears to be a common characteristics for metal supported-silicene as shown in Figs. 4 and 9(a)–9(f)[40,46] Fortunately, the destroyed Dirac cone can be restored by intercalating low concentration alkali metal atoms between silicene and substrates.[46] After intercalating K atoms for silicene on Pt, Au, and Al surfaces, the Si atoms are almost in the same plane ($\Delta = 0$ Å), and the zero Dirac cone is well recovered, with the estimated Fermi velocity on the order of 10^5 m/s, because of the recovered inversion symmetry of no buckling silicene (Figs. 9(g)–9(i)). While for the cases of silicene, with the intercalating of K atoms, on Ag, Mg, Cu, and Ir surfaces, the recovered Dirac cone is located at 0.40 eV∼0.78 eV below E_f, with an opened band gap of 0.15 eV∼0.40 eV, due to the built-in electric field induced by charge transfer (Figs. 9(j)–9(m)).

3. Silicene on non-metallic substrates

Devices of silicene require non-metallic substrates. Therefore, identifying non-metallic substrates suitable to host silicene is an important issue for realizing the devices based on silicene. We focus on a layered material with a honeycomb structure, such as insulating SiC and BN, transition-metal dichalcogenides MoX_2 and GaX (X = S, Se, Te), which are held together by weak vdW. The choice of these hexagonal layered templates for silicene is motivated by the following factors: (i) considerable band gaps (1 eV–6 eV); (ii) small lattice mismatch between silicene layer and substrates; (iii) pristine surfaces without out-of-plane dangling bonds, which may predict a weak interaction between silicene sheet and substrates.

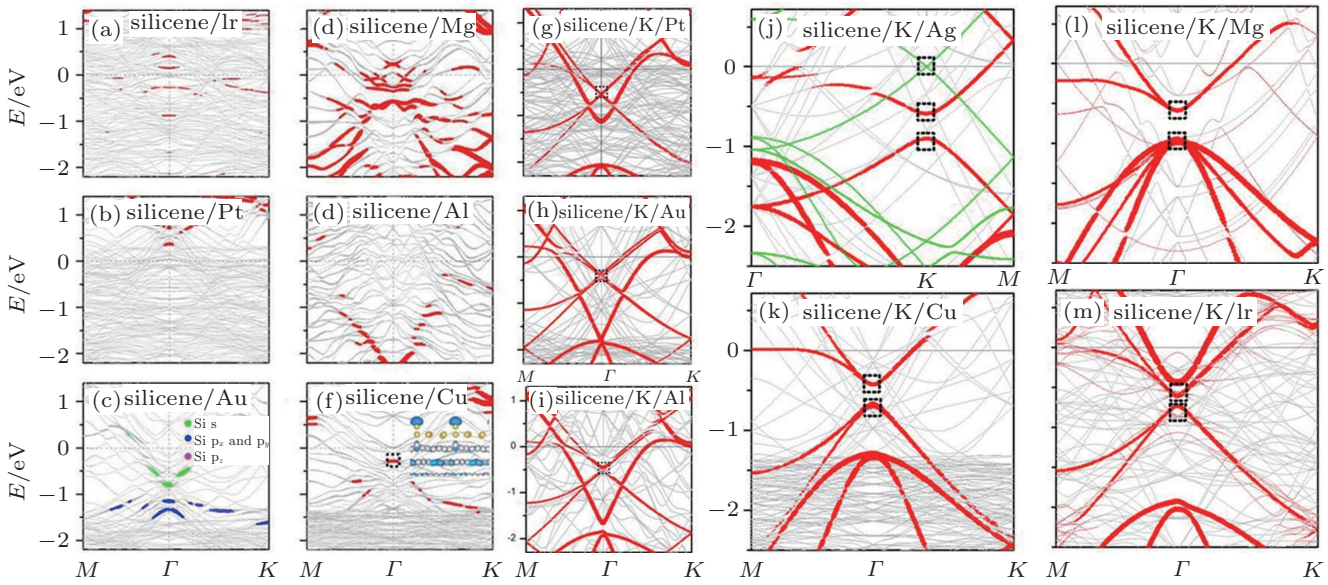


Fig. 9. (color online) (a)–(f) Band structures of epitaxial $\sqrt{3} \times \sqrt{3}$ silicene on various metallic Ir, Pt, Au, Mg, Al, Cu surfaces. (g)–(m) Band structures of epitaxial silicene on metals with K atoms intercalation. E_f is set to be zero. The red color indicates the states contributed from the Si atoms, and its thickness is related to the Si atom characteristic. Black squares in panels (g)–(m) indicate those states contributed from the π (π^*) bands of silicene (Reproduced with permission from Ref. [46]. Copyright 2014 Nature Publication Group).

3.1. Silicene on insulating BN/SiC surface

Recent first principles calculations proposed that the outstanding properties like the Dirac cone of silicene should be retained on hexagonal ML boron nitride (h-BN) and hydrogenated SiC (0001) surface.[6,24] The phases of (2×2)silicene/(3×3)BN and (4×4)silicene/(5×5)SiC (0001) are constructed because of their small Δa values of 2.04% and 0.08%, respectively. The honeycomb structure of silicene is maintained with a large d_0 (about 3 Å) on insulating BN and SiC substrates as shown in Fig. 10. This d_0 is comparable to that for graphene/BN system (3.22 Å) and is larger than that for silicene/metals. This large d_0 leads to a small E_b of 0.07 eV∼0.09 eV, indicating that the interaction between silicene and substrates is rather weak and can be viewed as vdW type. The weak vdW interaction results in small Δ of about 0.50 Å for silicene on BN and SiC, which is very close to the free-standing silicene buckling (0.44 Å). Therefore, the Dirac cones of silicene can be highly expected to be on these insulating hexagonal templates.

Furthermore, the original linear dispersion band of silicene is clearly preserved on the ML h-BN and Si-terminated SiC (0001) surface as shown in Figs. 10(e) and 10(f). It must be noted that the gapped Dirac cone is nearly at E_f (without any doping) in the band gaps of the two insulating substrates.[24,56] By contrast, for the silicene/C–SiC system, the supported-silicene becomes metallic, with the lower segment of the Dirac cone mixing up with the valence bands of the substrate in Fig. 10(g). The difference in band structures between these combined systems is also verified by the partial charge densities analyses, which concentrate on silicene near E_f for silicene/BN and silicene/Si–SiC, but distribute widely into the substrates for silicene/C–SiC.

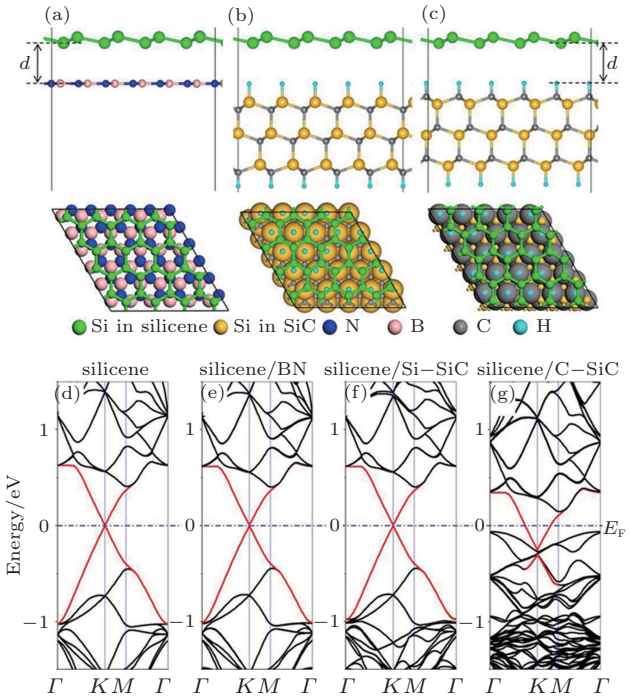


Fig. 10. (color online) Side (upper) and top (lower) views of the atomic configurations of (a) silicene/BN, (b) silicene/Si–SiC, (c) silicene/C–SiC hybrid systems. The corresponding electronic band structures of (d) silicene, (e) silicene/BN, (f) silicene/Si–SiC, (g) silicene/C–SiC. The red lines refer to the π-bands of silicene in different configurations (Reproduced with permission from Ref. [24]. Copyright 2013 American Chemical Society).

The physical mechanisms for the cases in Fig. 10 have been further explored. The different substrate effects are attributed to the different work functions,[24] i.e., the absolute positions of the valence band maximum (VBM) and conduction band minimum (CBM), of the substrates. The CBM (or VBM) of silicene is slightly 0.1 eV lower than the VBM of

C–SiC substrate, so that the charge will transfer from C–SiC substrate to silicene. The value of E_f of the hybrid system is thus higher than that of free-standing silicene, and the silicene in the hybrid system becomes metallic. On the contrary, for the silicene/BN and silicene/Si–SiC systems, the CBM of silicene is located in the gap region between BN and Si–SiC, resulting in a little charge transfer between silicene and the substrates. Consequently, the conical point of the Dirac cone in silicene is preserved at E_f, with small opened band gaps of 4 meV on BN and 3 meV on Si–SiC.

3.2. Silicene on semiconducting MoX_2 (X = S, Se, Te) and WSe_2 surfaces

Three different possible atomic arrangements of silicene layer (AAA stacking, intermediate position, and ABA stacking) on the top of MoX_2 (X = S, Se, Te) have been studied.[25,57,58] A large d_0 (3.0 Å∼3.5 Å) and a small E_b (10 meV–100 meV) suggest that there exists a vdW interaction between silicene and MoX_2. As given in Table 2, as Δa decreases from 18% to 9%, Δ decreases from 1.9 Å for silicene/MoS_2 to 0.7 Å for silicene/$MoTe_2$. Thus, the larger the lattice mismatch, the larger the supported-silicene buckling is. Usually, a large buckling suggests that there exists a strong interaction between silicene and substrates, which can enhance the possibility of losing Dirac cone. A large Δa is unfavorable for silicene epitaxial growth in experiment either.

It is noted that Δ of silicene on bulk MoS_2 is very close to the value for highly buckled free-standing (2.00 Å) silicene structure. Highly buckled silicene is predicted to be metallic and has several bands across E_f.[1] The energy band structure and the local density of states (Figs. 11(a) and 11(b)) confirm the metallic nature of silicene on bulk MoS_2. The gap of MoS_2 substrate is preserved, and all the electronic states near E_f are contributed from Si atoms. This clearly verifies that the vdW type of silicene/MoS_2 interaction almost has no hybridization between silicene and substrates. It is noted that the Δa between 4×4 silicene and 5×5 ML MoS_2 is rather small (2.42%).[59] In this case, the Δ of silicene on ML MoS_2 is 0.56 Å, close to the value for low buckled free-standing silicene structure. The supported-silicene is slightly p-doped and basically maintains its linear energy dispersion as shown in the corresponding electronic band structures and PDOS (Figs. 11(c) and 11(d)). The sublattice symmetry broken induces a small band gap (70 meV) at the Dirac cone. The band gap could be further tuned by an external electric field.

The band analyses are performed for silicene on $MoSe_2$ and $MoTe_2$ in Fig. 11. Interestingly, silicene on bulk $MoTe_2$ in Fig. 11(e) is a zero-gap semiconductor, preserving its Dirac cones at the K point. However, silicene on ML $MoTe_2$ is slightly doped by electrons and becomes metallic (Fig. 11(f)), with the band gap of the Dirac cone slightly opened because the inversion symmetry of silicene is destroyed by the charge transfer between silicene and ML $MoTe_2$.[8,46] Besides, other energy bands also share the same energy with the Dirac cone. In Fig. 11(g), silicene is moderately doped by electron on bulk $MoSe_2$, with a larger band gap near the Dirac cone. The geometrical structures and electronic structures for silicene on two MoX_2 layers in the same atomic configuration are nearly the same as the cases of silicene on ML MoX_2.[25]

Table 2. Structure parameters of the silicene on different non-metallic substrates. E_g is the theoretical band gap of the studied substrates (bulk phase), W is the work function of substrates in ML phase, E_D is the band gap near the Dirac cone, and ΔE_f is the energy shift of Dirac cone with respect to E_f.

	a/Å	Δa/%	E_g/eV	Δ/Å	d_0/Å	E_b/eV	W/eV	Dirac cone	E_D/meV	ΔE_f/meV
BN[24]	2.51	2.0	4.44	0.43∼0.51	3.23	0.09	5.86	Yes	4	0
Si–SiC[24]	3.08	0.1	2.42	0.5	2.73	0.07	5.54	Yes	3	0
C–SiC[24]	3.08	0.1	2.51	0.50	2.71	0.08	4.49	No	–	–
MoS_2[25,59]	3.16	18.3 (bulk) 2.42 (ML)	1.20 (bulk) 1.84 (ML)	1.90 0.56	3.00 2.93	0.10 0.12	5.12 5.36	No Yes	– 70	– 35
$MoSe_2$[25]	3.30	14.7	1.10	1.00	3.0∼3.5	0.01	4.52	No	–	–
$MoTe_2$[25]	3.52	9.0	1.00	0.70	3.0∼3.5	0.01	4.20	Yes	0	0
WSe_2[26]	3.31	0.6		0.51	3.20	0.12	4.37	Yes	320	150
GaS[25,60]	3.58	7.5	2.50	0.70	4.5∼5.0 (bulk) 3.1∼3.8(ML)	0.07	–	Yes	170	0
GaSe[25]	3.74	3.4	2.00	0.55	–	0.07	–	Yes	0	0
GaTe[25]	4.10	–5.9	1.80	0.30	–	0.07	–	Yes	0	0
$MgCl_2$[61]	3.62	–1.9	6.00	0.55	3.41	0.05	–	Yes	9∼41	2∼19
$MgBr_2$[61]	3.83	1.0	4.80	0.49	3.23	0.06	–	Yes	13∼64	2∼24
MgI_2[61]	4.15	2.9	3.60	0.40	3.19	0.06	–	Yes	1∼90	0∼39
AlN[62]	3.11	19.0	4.80	0.22	–	–	–	Yes	0	0
ZnS[63]	3.81	2.3	3.06	–	3.33	–	–	No	–	–
CaF_2[64]	3.88	0.5	–	0.43	2.70	–	–	Yes	52	0

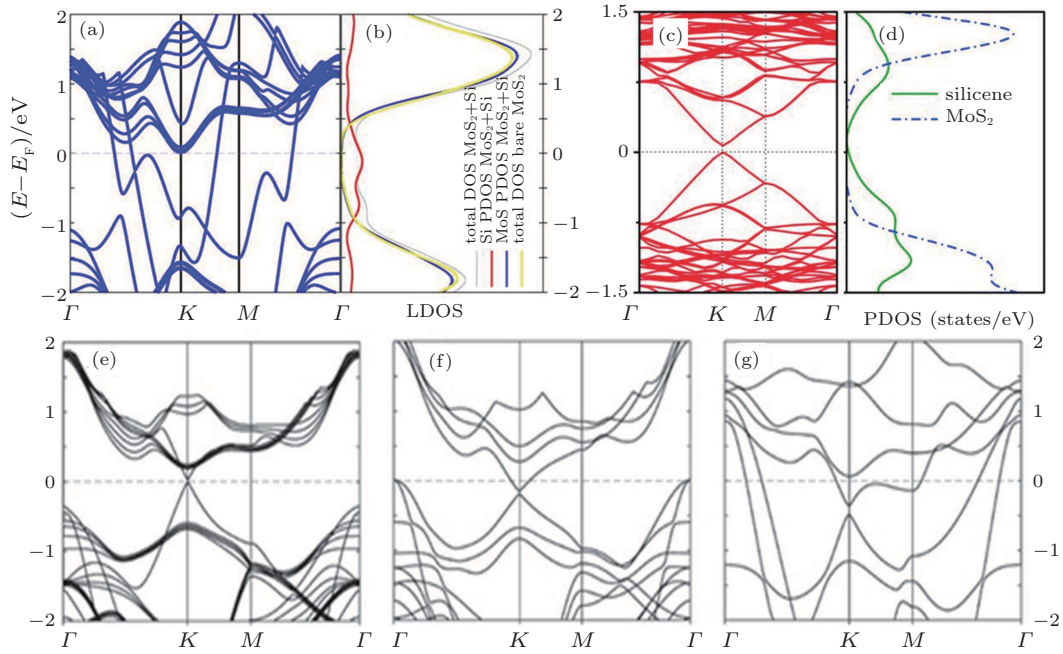


Fig. 11. (color online) Electronic band structure (a) and local density of states (b) of silicene on bulk MoS_2. Electronic band structure (c) and partial density of states (d) of silicene on monolayer MoS_2. Band structures of silicene on (e) bulk $MoTe_2$, (f) monolayer $MoTe_2$, and (g) $MoSe_2$. Reproduced with permissions from Refs. [25] and [59] (Copyright 2014 Institute of Physics and Royal Society of Chemistry).

WSe_2 has a smallest value of Δa with silicene (0.6%) among the transition metal dichalcogenides.[26] Because of their instabilities, the combined system varies from metallic state to semiconducting state with a band gap up to 0.3 eV, but accompanied with a well preserved Dirac cone. When WSe_2 is doped by S and Te, the combined heterosheet becomes stable, with atomic and electronic structures nearly being the same as those for silicene on pristine WSe_2. However, high-buckled silicene on WSe_2 has a Δ value of 1.3 Å, a small d_0 of 2.55 Å, and a large E_b of 195 meV, indicating strong interaction between silicene and substrates compared with the case of low-buckled silicene (Δ of 0.51 Å, d_0 of 3.20 Å, and E_b of 120 meV).

3.3. Silicene on GaX (X = S, Se, Te) surfaces

GaX (X = S, Se, Te) is another class of chalcogenide compounds with a vdW layered hexagonal structure. The cell parameters are larger for GaX and the Δa values (3%∼8%) with free-standing silicene are smaller than those for MoX_2.[25,60] A small E_b (0.07 eV) suggests a weak vdW type of silicene/GaX. The Δ values are small, ranging from 0.30 Å∼0.70 Å. The d_0 values for silicene on bulk GaX (4.5 Å∼5 Å) are much larger than those for silicene on ML GaX (3.1 Å∼3.8 Å), similar to the case of MoX_2. It appears that the interaction between the silicene and GaX and MoX_2 can be enhanced by reducing the layer number.

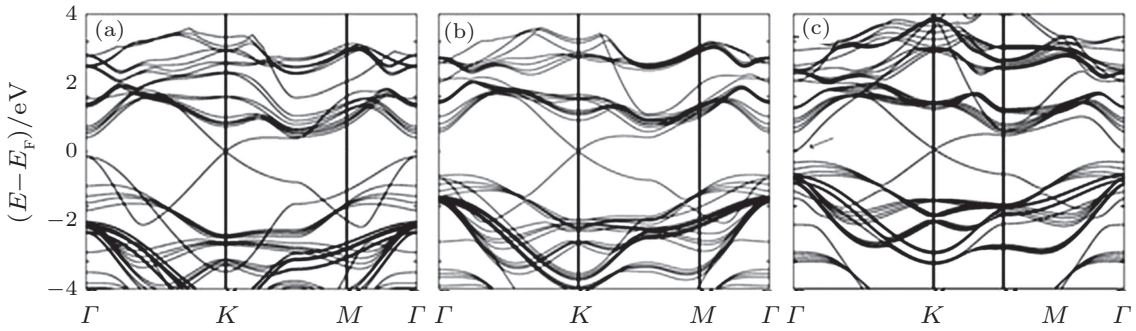


Fig. 12. Electronic band structures of the silicene layer on (a) bulk GaS, (b) GaSe, and (c) GaTe. The arrow in panel (c) indicates the band crossing E_f (Reproduced with permission from Ref. [25]. Copyright 2014 Institute of Physics).

Figure 12 displays the electronic band structure of silicene/bulk GaX.[25] Remarkably, both silicene/bulk GaS and silicene/bulk GaSe preserve the linear band dispersion crossing E_f at the K point, with band gaps (0.7 eV and 1.5 eV, respectively) at the Γ point. These two combined systems are expected to be gapless semiconductors, just like free-standing silicene. Therefore, these heterosheets belong to the Dirac system, possessing outstanding properties like the high Fermi ve-

locity and carrier mobility. Although the Dirac cone is preserved for silicene/bulk GaTe, there is a band touching E_f at the Γ point, and this will mask the intrinsic properties of the Dirac carrier. On condition that the sandwiched configurations have the same stacking modes as the bulk structure, there is nearly no difference between ML GaTe/silicene/ML GaTe (silicene in-between two GaTe layers) and silicene/bulk GaTe. The gapless Dirac cone in silicene/bulk GaS turns into a gapped (about 0.1 eV) one in ML GaS/silicene/ML GaS due to the interlayer charge distribution. Furthermore, this gap value of ML GaS/silicene/ML GaS can be modulated by an external electric field and strain.[60]

3.4. The silicene on the other non-metallic substrates (MgX_2/AlN/ZnS/CaF$_2$)

Arranged on hexagonal lattice, ML MgX_2 (X = Cl, Br, and I) are insulators with calculated band gaps ranging from 3.6 eV to 6.0 eV.[61] The lattice mismatches between ML MgX_2 and silicene are smaller than 2.9%. Three high symmetry configurations of silicene on ML MgX_2 (0001) have been checked and turned out to be almost degenerate. All silicene/ML MgX_2 heterosheets show small Δ (0.39 Å∼0.55 Å), large d_0 (3.23 Å∼3.75 Å), and small E_b (33 meV∼88 meV), a typical weak vdW interaction. The band structures of silicene on ML MgX_2 (0001) for three configurations are displayed in Fig. 13.[61] In each case, the supported-silicene is minor p doping and preserves its intrinsic electronic properties well, such as the Dirac-cone-like energy band and high Fermi velocity (estimated 10^5 m/s). Owing to the charge redistribution at the interface of heterosheets, small band gaps are opened in the supported-silicene (1 meV∼90 meV). The opened band gap can be further modulated by an external electric field and strain, and increase (decrease) almost linearly with electric field (strain) increasing.[61]

As is well known, bulk AlN is wurtzite phase with an experimental semiconducting band gap of 6.5 eV, while ultrathin AlN prefers to have hexagonal honeycomb lattice with a smaller energy gap of 4.5 eV. Houssa *et al.* predicted that silicene inserted into ultrathin AlN (0001) stacks preserves its graphene-like electronic properties because of the weak vdW layer interaction and the low silicene buckling (0.22 Å).[62] Like AlN, semiconducting ZnS is also a wurtzite phase in bulk and shows hexagonal honeycomb lattice in layers. The forming bonds cause charges to transfer between silicene and ZnS, leading to a semiconducting combined system, with a large opened indirect band gap of 0.7 eV. The Dirac-cone-like energy dispersion is thus unfortunately destroyed.[63] While on CaF_2 (111), the supported-silicene preserves the original undoped Dirac cone well, with a small opened band gap of 52 meV.[64]

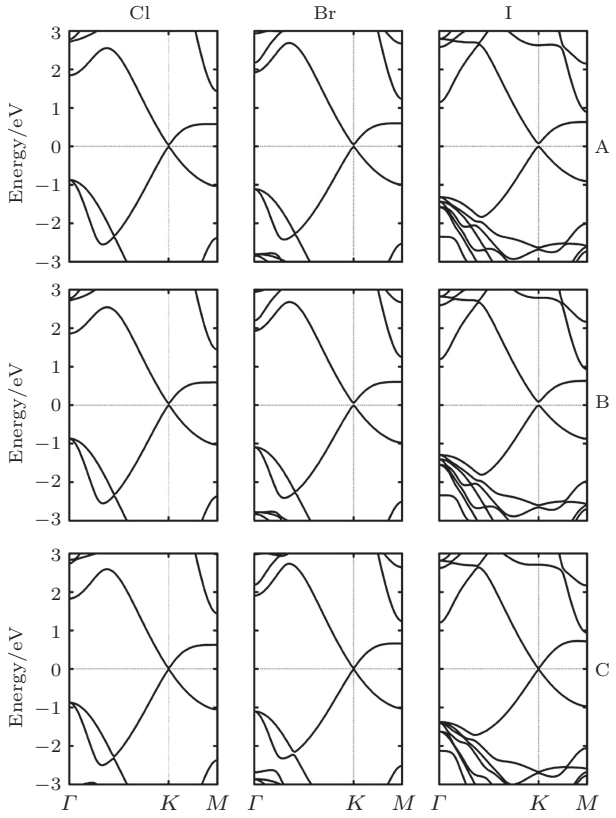


Fig. 13. Band structures of silicene on MgX_2 (0001) (X = Cl, Br, and I) for configurations A–C. The E_f is set to be zero. Reproduced with permission from Ref. [61]. Copyright 2014 American Chemical Society.

4. Conclusion and outlook

In Section 2, the electronic properties of epitaxial silicene layers on metallic substrates are summarized in Table 1. The lattice mismatch ranges from 1% to 15%, which does not change the conclusion about the Dirac cone is present or absent in metal-supported silicene. Owing to the strong interaction between silicene and most metallic substrates, metal-supported silicene loses its original linear energy dispersion, except for graphene, Ca, and Pb substrates. On these three substrates, the weak vdW interaction between silicene and substrates can be obtained, leading to gapped silicene-derived Dirac cone with slightly n-doped. For the serious destruction of the Dirac cone in metal-supported silicene, the Dirac cone can be fortunately restored by intercalating low concentration alkali metal atoms between silicene and metallic substrates.

In Section 3, we discussed the electronic properties of epitaxial silicene layers on non-metallic substrates as shown in Table 2. Because of pristine substrate surface (no dangling bond), weak vdW interaction between silicene and layered substrates, and appropriate work function, most supported-silicene can preserve its original Dirac cone, with opened small band gap (0 meV∼320 meV) and slightly doped. The opened band gap can be further modulated by an external electric field and strain, with the linear band dispersion and high Fermi velocity (10^5 m/s). The lattice mismatch and absolute

band edge of substrates play vital role in the changing of Dirac cone. Therefore, the hexagonal layered 2D semiconductors and insulators have the advantage to host the Dirac particles compared with the metals.

However, so far low-buckled silicene has been successfully synthesized only on metallic Ag (111), ZrB_2 (0001), Ir (111), and ZrC (111) templates, which completely destroy the original Dirac cone of silicene due to the strong interaction between silicene and templates as indicated by most theoretical and experimental investigations. Weak vdW interaction is thus desired between silicene and templates. Metallic graphene, Ca, Pb, and most non-metallic hexagonal layered templates are predicted to host the linear band dispersion of silicene. The lattice mismatch and absolute band edge of substrates play vital roles in the changing of the Dirac cone. Moreover, high-buckled silicene has been successfully synthesized on MoS_2 surface very recently,[21] suggesting that non-metallic templates have the potential to grow silicene experimentally. This experimental breakthrough is expected to pave a way for synthesizing the silicene on 2D layered non-metallic substrates with preserving the intrinsic properties of silicene.

References

[1] Cahangirov S, Topsakal M, Aktürk E, Şahin H and Ciraci S 2009 *Phys. Rev. Lett.* **102** 236804
[2] Li X, Mullen J T, Jin Z, Borysenko K M, Buongiorno Nardelli M and Kim K W 2013 *Phys. Rev. B* **87** 115418
[3] Shao Z G, Ye X S, Yang L and Wang C L 2013 *J. Appl. Phys.* **114** 093712
[4] Quhe R, Zheng J, Luo G, Liu Q, Qin R, Zhou J, Yu D, Nagase S, Mei W N, Gao Z and Lu J 2012 *NPG Asia Mater.* **4** e6
[5] Drummond N D, Zólyomi V and Fal'ko V I 2013 *Phys. Rev. B* **85** 075423
[6] Ni Z, Liu Q, Tang K, Zheng J, Zhou J, Qin R, Gao Z, Yu D and Lu J 2012 *Nano Lett.* **12** 113
[7] Quhe R G, Fei R, Liu Q, Zheng J, Li H, Xu C, Ni Z, Wang Y, Yu D, Gao Z and Lu J 2012 *Sci. Rep.* **2** 853
[8] Ni Z G, Zhong H, Jiang X, Quhe R G, Luo G, Wang Y, Ye M, Yang J, Shi J and Lu J 2014 *Nanoscale* **6** 7609
[9] Zhu Y F, Dai Q Q, Zhao M and Jiang Q 2013 *Sci. Rep.* **3** 1524
[10] Tao L, Cinquanta E, Chiappe D, Grazianetti C, Fanciulli M, Dubey M, Molle A and Akinwande D 2015 *Nat. Nanotech.* **10** 227
[11] Gmitra M, Konschuh S, Ertler C, Ambrosch-Draxl C and Fabian J 2009 *Phys. Rev. B* **80** 235431
[12] Liu C C, Feng W and Yao Y 2011 *Phys. Rev. Lett.* **107** 076802
[13] Ezawa M 2012 *Phys. Rev. Lett.* **109** 055502
[14] Pan H, Li Z, Liu C C, Zhu G, Qiao Z and Yao Y 2014 *Phys. Rev. Lett.* **112** 106802
[15] Tsai W F, Huang C Y, Chang T R, Lin H, Jeng H T and Bansil A 2013 *Nat. Commun.* **4** 1500
[16] Vogt P, De Padova P, Quaresima C, Avila J, Frantzeskakis E, Asensio M C, Resta A, Ealet B and Le Lay G 2012 *Phys. Rev. Lett.* **108** 155501
[17] Feng B, Ding Z, Meng S, Yao Y, He X, Cheng P, Chen L and Wu K 2012 *Nano Lett.* **12** 3507
[18] Fleurence A, Friedlein R, Ozaki T, Kawai H, Wang Y and Yamada-Takamura Y 2012 *Phys. Rev. Lett.* **108** 245501
[19] Meng L, Wang Y, Zhang L, Du S, Wu R, Li L, Zhang Y, Li G, Zhou H, Hofer W A and Gao H J 2013 *Nano Lett.* **13** 685
[20] Aizawa T, Suehara S and Otani S 2014 *J. Phys. Chem. C* **118** 23049
[21] Chiappe D, Scalise E, Cinquanta E, Grazianetti C, van den Broek B, Fanciulli M, Houssa M and Molle A 2014 *Adv. Mater.* **26** 2096
[22] Pflugradt P, Matthes L and Bechstedt F 2014 *New J. Phys.* **16** 075004
[23] Paszkowska A and Krawiec M 2015 *Phys. Chem. Chem. Phys.* **17** 2246
[24] Liu H, Gao J and Zhao J 2013 *J. Phys. Chem. C* **117** 10353
[25] Scalise E, Houssa M, Cinquanta E, Grazianetti C, van den Broek B, Pourtois G, Stesmans A, Fanciulli M and Molle A 2014 *2D Mater.* **1** 011010
[26] Zhu J and Schwingenschlogl U 2015 *J. Mater. Chem. C* **3** 3946
[27] Cai Y, Chuu C P, Wei C M and Chou M Y 2013 *Phys. Rev. B* **88** 245408
[28] Liu F, Liu C C, Wu K, Yang F and Yao Y 2013 *Phys. Rev. Lett.***111** 066804
[29] Chen L, Feng B and Wu K 2013 *Appl. Phys. Lett.* **102** 081602
[30] Kara A, Léandri C, Dávila M E, De Padova P, Ealet B, Oughaddou H, Aufray B and Le Lay G 2009 *J. Supercond. Nov. Magn.* **22** 259
[31] Gao J and Zhao J 2012 *Sci. Rep.* **2** 861
[32] Chiappe D, Grazianetti C, Tallarida G, Fanciulli M and Molle A 2012 *Adv. Mater.* **24** 5088
[33] Lin C H, Arafune R, Kawahara K, Kanno M, Tsukahara N, Minamitani E, Kim Y, Kawai M and Takagi N 2013 *Phys. Rev. Lett.* **110** 076801
[34] Lin C H, Arafune R, Kawahara K, Tsukahara N, Minamitani E, Kim Y, Takagi N and Kawai M 2012 *Appl. Phys. Express* **5** 045802
[35] Jamgotchian H, Colignon Y, Hamzaoui N, Ealet B, Hoarau J Y, Aufray B and Biberian J P 2012 *J. Phys: Condens. Matter* **24** 172001
[36] Lalmi B, Oughaddou H, Enriquez H, Kara A, Vizzini S, Ealet B and Aufray B 2010 *Appl. Phys. Lett.* **97** 223109
[37] Chen L, Liu C C, Feng B, He X, Cheng P, Ding Z, Meng S, Yao Y and Wu K 2012 *Phys. Rev. Lett.* **109** 056804
[38] Chen L, Li H, Feng B, Ding Z, Qiu J, Cheng P, Wu K and Meng S 2013 *Phys. Rev. Lett.* **110** 085504
[39] Cahangirov S, Audiffred M, Tang P, Iacomino A, Duan W, Merino G and Rubio A 2013 *Phys. Rev. B* **88** 035432
[40] Yuan Y, Quhe R G, Zheng J, Wang Y, Ni Z, Shi J and Lu J 2014 *Physica E* **58** 38
[41] Gori P, Pulci O, Ronci F, Colonna S and Bechstedt F 2013 *J. Appl. Phys.* **114** 113710
[42] Guo Z X, Furuya S, Iwata J I and Oshiyama A 2013 *J. Phys. Soc. Jpn.* **82** 063714
[43] Guo Z X, Furuya S, Iwata J I and Oshiyama A 2013 *Phys. Rev. B* **87** 235435
[44] Pflugradt P, Matthes L and Bechstedt F 2014 *Phys. Rev. B* **89** 035403
[45] Wang Y P and Cheng H P 2013 *Phys. Rev. B* **87** 245430
[46] Quhe R G, Yuan Y, Zheng J, Wang Y, Ni Z, Shi J, Yu D, Yang J and Lu J 2014 *Sci. Rep.* **4** 5476
[47] Arafune R, Lin C L, Nagao R, Kawai M and Takagi N 2013 *Phys. Rev. Lett.* **110** 229701
[48] Resta A, Leoni T, Barth C, Ranguis A, Becker C, Bruhn T, Vogt P and Le Lay G 2013 *Sci. Rep.* **3** 2399
[49] Guo Z X and Oshiyama A 2014 *Phys. Rev. B* **89** 155418
[50] Lee C C, Fleurence A, Friedlein R, Yamada-Takamura Y and Ozaki T 2013 *Phys. Rev. B* **88** 165404
[51] Lee C C, Fleurence A, Yamada Takamura Y, Ozaki T and Friedlein R 2014 *Phys. Rev. B* **90** 075422
[52] Wei W, Dai Y, Huang B, Whangbo M H and Jacob T 2015 *J. Phys. Chem. Lett.* **6** 1065
[53] Hu W, Li Z and Yang J 2013 *J. Chem. Phys.* **139** 154704
[54] Neek Amal M, Sadeghi A, Berdiyorov G R and Peeters F M 2013 *Appl. Phys. Lett.* **103** 261904
[55] Wang Y, Ni Z, Liu Q, Quhe R G, Zheng J, Ye M, Yu D, Shi J, Yang J and Lu J 2015 *Adv. Funct. Mater.* **25** 68
[56] Gao N, Li J C and Jiang Q 2014 *Chem. Phys. Lett.* **592** 222
[57] Houssa M, Scalise E, van den Broek B, Lu A, Pourtois G, Afanas'ev V V and Stesmans A 2015 *J. Phys. Chem. Solids* **574** 012015
[58] Li L and Zhao M 2014 *J. Phys. Chem. C* **118** 19129
[59] Gao N, Li J C and Jiang Q 2014 *Phys. Chem. Phys.* **16** 11673
[60] Ding Y and Wang Y 2013 *Appl. Phys. Lett.* **103** 043114
[61] Zhu J and Schwingenschlogl U 2014 *ACS Appl. Mater. Interfaces* **6** 11675
[62] Houssa M, Pourtois G, Heyns M M, Afanasév V V and Stesmans A 2011 *J. Electrochem. Soc.* **158** H107
[63] Houssa M, van den Broek B, Scalise E, Pourtois G, Afanasév V V and Stesmans A 2013 *Phys. Chem. Chem. Phys.* **15** 3702
[64] Kokott S, Pflugradt P, Matthes L and Bechstedt F 2014 *J. Phys: Condens. Matter* **26** 185002